

Joint 3D inversion of time- and frequency-domain airborne electromagnetic data

David Sunwall* and Leif Cox, *TechnoImaging*; Michael Zhdanov, *University of Utah and TechnoImaging*

Summary

We present a method of 3D joint inversion of frequency-domain and time-domain airborne electromagnetic (AEM) data. The method is based on the concept of a moving sensitivity domain, which makes it possible to invert large scale AEM surveys to 3D conductivity models. Frequency-domain AEM data have better resolution for near-surface structures, while time-domain data can resolve deeper geologic targets. By combining these two methods in joint inversion, we produce well resolved images of an entire geological section under investigation. There are many mature areas in mining and petroleum producing provinces where both frequency-domain and time-domain airborne surveys already exist. Reprocessing these areas with the proposed joint inversion scheme may lead to improved images, better understanding, and a more accurate geologic model.

Introduction

Since the advent of airborne electromagnetic (AEM) techniques, AEM acquisition technology has, until recently, outpaced the development of accurate and efficient inversion of AEM data. Before 2007, only pseudo-3D conductivity models, from a variety of 1D inversion methods, were derived from entire large-scale AEM surveys. To reduce computational and memory requirements associated with large-scale inversion of AEM data, Cox and Zhdanov (2007) introduced a moving-footprint concept into their AEM inversion algorithm. A moving footprint takes advantage of the fact that the received signal of an AEM system is only influenced by a domain, termed the sensitivity domain, which is much smaller than the entire survey domain. Using the moving footprint approach, 3D inversion of entire AEM data sets suddenly became practical, reliable, rapid, and able to delineate deposit-scale features (Cox et al., 2010, 2012). AEM surveys are conducted either in the frequency-domain (FD) or time-domain (TD). The near surface is typically imaged better by FD surveys because the highest frequency used is generally above 100 kHz, as in a RESOLVE system. However, FD systems are unable to image as deep as TD systems and in general cannot see through conductive cover. FD surveys are often relegated to environmental applications where typical target depths are less than 150 m, whereas TD surveys are often used for mineral exploration where the desired imaging depth may be in excess of 500 m. It is natural to ask if these two methods can be combined to create high resolution images from the near surface (<5m) to greater depths (>500m).

In this paper, we describe a 3D joint inversion scheme for FD and TD AEM data. A synthetic model is presented showing the two airborne methods can be combined into a single joint-inversion scheme which has high resolution in the near surface combined with information at depth. We also demonstrate the effectiveness of joint inversion on RESOLVE and SkyTEM field data collected near Bookpurnong, South Australia.

Inversion Methodology

As described in Zhdanov (2009) and Cox et al. (2010, 2012), the forward modeling is based on the rigorous 3D contraction integral-equation method (Hursan and Zhdanov, 2002). For the modeling of a moving sensitivity domain, the volume of interest for a given source is defined as the subdomain of the 3D earth model encapsulated in the AEM system's footprint, and only sensitivities within the sensitivity domain need to be calculated. Because AEM inverse solutions are nonunique and unstable, we use regularized inversion based on the minimization of the Tikhonov parametric functional,

$$P^\alpha(\sigma) = \varphi(\sigma) + \alpha \|W_m(\sigma - \sigma_{appr})\|^2 \rightarrow \min, \quad (1)$$

In equation (1), α is the regularization parameter, and $\varphi(\sigma)$ is the misfit functional (or residual errors) between the predicted, $d_{pre} = A(\sigma)$, and observed, d_{obs} , data:

$$\varphi(\sigma) = \|W_d(A(\sigma) - d_{obs})\|^2, \quad (2)$$

where A is the nonlinear forward operator, σ is the N_m length vector of conductivities, d_{obs} is the N_d length vector of observed data, σ_{appr} is the N_m length vector of a priori conductivities, and $\|\dots\|^2$ denotes the respective Euclidean norm. Data and model weights are W_d and W_m , respectively. Data weights are included because the magnitudes within and between FD and TD surveys vary by many orders of magnitude. To account for both the magnitude and uncertainty in every data point, we choose to set:

$$W_{d,i} = \frac{1}{\varepsilon_i}, \quad (3)$$

where ε_i the estimated error in the corresponding data point. The minimization of equation (1) is then solved using a reweighted regularized conjugate gradient (RRCG) method (Zhdanov, 2002). The data weights are simply given by equation (3), which includes both FD and TD errors. The Fréchet derivative (sensitivity) matrix, F is a concatenation of FD and TD Fréchet derivatives:

Joint 3D inversion of time- and frequency-domain airborne electromagnetic data

$$F = \begin{bmatrix} F^{FD} \\ F^{TD} \end{bmatrix}. \quad (4)$$

The model weights are given by:

$$W_m = \text{diag}(F^*F)^{1/4}, \quad (5)$$

where (*) denotes a transposed complex conjugate matrix. Thus, any weighting discrepancies between FD and TD data can be accounted for by carefully selecting errors for the joint data-weighting matrix, W_d . Model weights are still derived from the Fréchet matrix which already accounts for both FD and TD forward operators. No modifications are needed for the RRCG method for the joint inversion compared to FD- or TD-only inversion. We also follow an iterative process of updating electric fields between runs of RRCG minimization as described by Cox and Zhdanov (2008).

Synthetic Model Study

This model study is intended to compare the individual and joint 3D inversion results from separate simulations of a FD survey and TD survey. Using the same model, two synthetic data sets were generated using RESOLVE (FD) and HeliTEM (TD) configurations. The model consists of four conductors ($5 \Omega \cdot \text{m}$) and two resistors ($2000 \Omega \cdot \text{m}$) in a $100 \Omega \cdot \text{m}$ homogeneous half-space (Figure 1a). This model includes simplistic yet ideal targets for both FD and TD surveys. Note that Figure 1 only displays cross sections of 3D models, and the model domain, conductors, and resistors have a strike of 425 m parallel to the direction in and out of the page.

Three survey lines were simulated for both RESOLVE and HeliTEM systems. The survey lines run EW (perpendicular to the strike of the conductive and resistive bodies) and are spaced 50 m apart. Soundings were taken every 12 m along the survey lines, and a total of 150 data points were simulated per each survey. Transmitter flight heights were constant at 35 m.

The parameters for this simulated RESOLVE survey are shown in Table 1. The RESOLVE data were inverted for a 3D conductivity model with approximately 18,360 cells that were 15 m by 25 m in the respective EW/NS directions, and varied from 1 m thick (model's top layer) to 26 m thick (model's bottom layer) in the vertical direction. The sensitivity domain of the RESOLVE system was set to 500 m by 500 m. The a priori model for 3D inversion consisted of a homogeneous $100 \Omega \cdot \text{m}$ half-space. The RESOLVE-only inversion recovered the two, small, and shallow conductors and the medium-sized, 24 m-deep conductor (Figure 1b). For the conductors which were

imaged, the RESOLVE inversion successfully placed the top of the conductors at the correct depths but did not accurately recover the conductors' thicknesses. This inability to recover thickness was especially apparent in the shallow conductors which are much thicker than the true model. The shallow resistors and large 135 m deep conductor were not imaged.

Table 1: RESOLVE survey parameters.

Frequency	Tx-Rx Orientation	Tx-Rx Separation
378 Hz	Horizontal coplanar	7.93 m
1,843 Hz	Horizontal coplanar	7.90 m
3,260 Hz	Vertical coaxial	9.06 m
8,180 Hz	Horizontal coplanar	7.94 m
40,650 Hz	Horizontal coplanar	7.95 m
128,510 Hz	Horizontal coplanar	7.93 m

The HeliTEM system was configured at a 30 Hz base frequency. The system recorded 30 channels (4 on-time, 26 off-time) of vertical (Z) and in line (X) data. HeliTEM data were inverted to the exact same inversion domain parameters as the RESOLVE inversion and using the same a priori model. The HeliTEM-only inversion recovered the medium-sized 24 m deep conductor and the large 135 m deep conductor, and recovered the vertical extent of the conductive bodies better than RESOLVE (Figure 1c). No small shallow conductors or resistors were imaged, except for a possible faint image of the small 4 m deep conductor located 355 m along the cross section.

Consistent with the RESOLVE-only and HeliTEM-only inversions, the joint inversion was run with the same inversion-domain parameters and same a priori model. The joint inversion recovered all conductors from the original model, including the deep conductor which FD-only inversion did not recover and the shallow conductors which TD-only inversion did not recover (Figure 1d). Additionally, the joint inversion did better recovering the thicknesses of the conductive bodies, especially for the shallow conductors. The inverted image combines the best qualities of the FD and TD inversions, plus improved the near surface resolution over what can be imaged over either inversion individually. The nature of FD surveys limits their ability to "see" through conductors. TD techniques have the advantage of deeper penetration, but their bandwidth limits the resolution. The joint inversion combines the advantages of resolution (FD) and penetration (TD), and the final inversion results are better representations of the true model.

Case study: Bookpurnong, Australia

Along the Murray River in South Australia, efforts are being made to better understand the relationship between hydrogeologic and salinization processes occurring within and near the floodplains of the Murray River. Especially

Joint 3D inversion of time- and frequency-domain airborne electromagnetic data

during seasons of drought, the salinization of groundwater, river water, and floodplain soil has a negative impact on floodplain vegetation. Saline soil and saline groundwater are ideal targets for high-resolution AEM methods, so, over the study area, RESOLVE (FD) data were collected in July 2005 and SkyTEM (TD) data were collected in August and September of 2006. The study area includes a 9-mile (14.5-km) section of the Murray River and its surrounding floodplain. At the time, these surveys were conducted coextensively to compare the relative effectiveness between RESOLVE and SkyTEM systems in the study area. These surveys were not conducted for the purpose of joint inversion; however, both systems were independently effective in locating areas of high salt concentration in the study area and are therefore suitable for joint inversion.

System configurations for the RESOLVE survey are shown in Table 2. Twenty six lines of RESOLVE data were collected at 100 m spacing. The SkyTEM system was configured at a 25 Hz base frequency for high-moment mode and 222 Hz for low-moment mode. In high-moment mode the system recorded 24 channels (all channels off-time) of vertical (Z) and in-line (X) data. In low-moment mode the system recorded 20 channels (4 on-time, 16 off-time) of vertical (Z) and in-line (X) data. Twenty nine lines of SkyTEM data were collected at 100 m spacing, and lines vary in length from 4.9 km to 6.9 km long. Nominal transmitter flight-height for this survey was ~60 m.

Table 2: RESOLVE survey parameters.

Frequency	Tx-Rx Orientation	Tx-Rx Separation
390 Hz	Horizontal coplanar	7.91 m
1,798 Hz	Horizontal coplanar	7.91 m
3,242 Hz	Vertical coaxial	8.99 m
8,177 Hz	Horizontal coplanar	7.91 m
39,470 Hz	Horizontal coplanar	7.91 m
132,700 Hz	Horizontal coplanar	7.91 m

As in the synthetic example, we inverted the RESOLVE and SkyTEM data independently and jointly. Figures 2a, 2b, and 2c show cross-sections of 3D models from the respective FD-only inversion, TD-only inversion, and joint inversion. The estimated data errors, which are used for data weighting, are shown in Table 3.

Final inversion results of these field data show similar characteristics observed in the synthetic inversions. For example in the joint inversion, notice the shallow-conductor/mid-depth-resistor/deep-conductor sequence (Figure 2d). The thin shallow conductor is imaged well by both FD- and TD-only inversions, but FD-only has difficulty seeing through the shallow conductor and recovering the conductor's thickness. Furthermore, FD data are unable to image the deep conductor. TD data image the deep conductor well but have difficulty clearly defining the resistor which is located, vertically, between the two

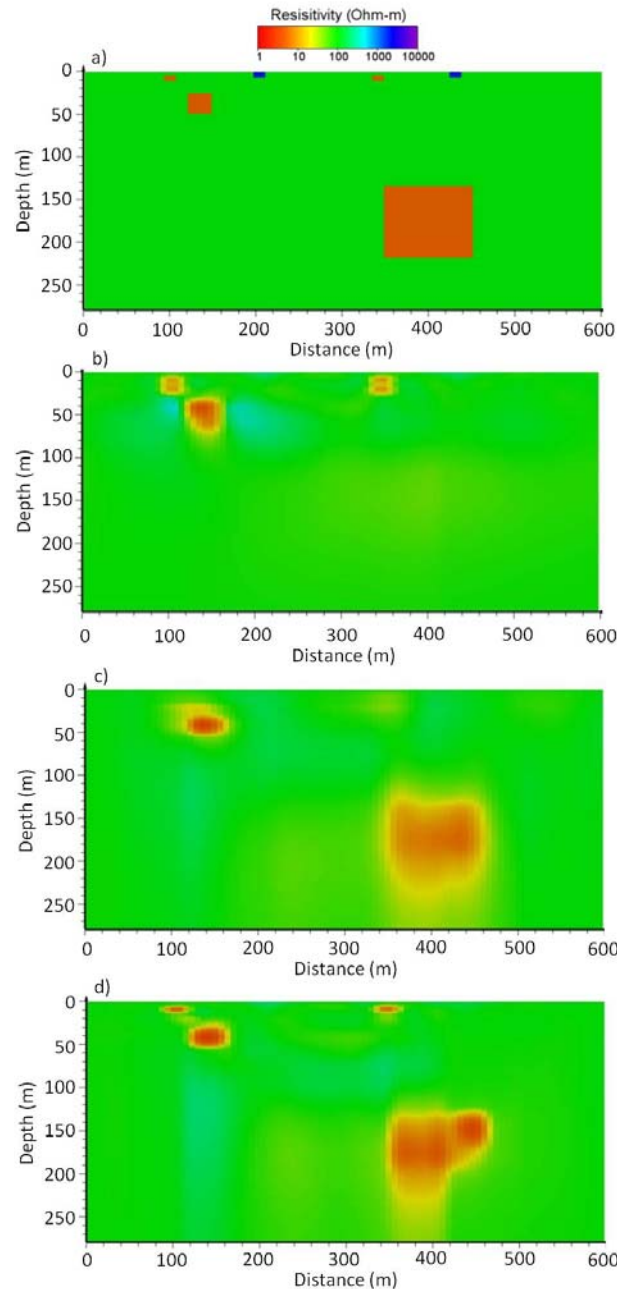


Figure 1: a) Model used to generate both RESOLVE and HeliTEM synthetic data. b) RESOLVE-only inversion. Notice only the two small, shallow conductors and the medium, 24 m deep conductor were recovered. c) HeliTEM-only inversion. Notice only the medium 24 m deep conductor and the large 135 m deep conductor were imaged. d) Joint inversion of RESOLVE and HeliTEM synthetic data. Notice all conductors have been successfully recovered.

Joint 3D inversion of time- and frequency-domain airborne electromagnetic data

Table 3: Estimated errors for Bookpurnong data

RESOLVE Channels	Absolute error (ppm)	Relative error (%)
390 Hz	5	5
1,798 Hz	10	5
3,242 Hz	10	8
8,177 Hz	15	5
39,470 Hz	20	5
132,700 Hz	30	5
SkyTEM Channels	Absolute error (nT/ A·s·m ²)	Relative error (%)
Low moment Z	0.01	15
High moment Z	0.001	15

conductors. Across all depths, joint inversion clearly delineates the conductor-resistor-conductor sequence, and overall joint inversion produces a better image compared to independent inversions of FD data or TD data.

Conclusions

FD and TD airborne surveys each have different advantages and disadvantages in what they can resolve. In general, the FD surveys have higher near-surface resolution, but cannot see through conductive material nor as deep as TD surveys. TD methods are able to penetrate to greater depths and through conductive overburden yet cannot capture near surface variations as well as FD surveys. By jointly inverting these two survey types, the conductivity model can be greatly improved. We have shown this in our synthetic example where joint inversion was able to image deep conductors that were not apparent in the FD inversion, while the near-surface joint showed an improvement over inverting either the FD or TD individually. Likewise, joint inversion of field data from the Bookpurnong irrigation district has imaged features in the near-surface and at depth that neither FD- nor TD-only inversions could produce independently. Also, by using a two-part error model and weighting each data point by its estimated error, each data point is fit to an appropriate level without the need for an artificial trade-off parameter in the misfit functional.

This latest development in 3D AEM inversion should increase the success of AEM-led exploration and decrease the risk involved in the development of new mineral deposits. There are many mature areas in mining and petroleum producing provinces where both TD and FD airborne surveys already exist. Reprocessing these areas with the proposed joint inversion scheme may lead to improved images, better understanding, and a more accurate geologic model.

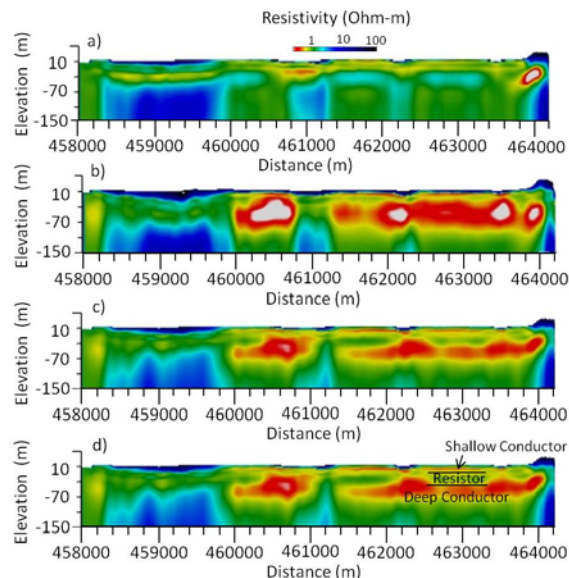


Figure 2: a) RESOLVE-only inversion of Bookpurnong data. b) SkyTEM-only inversion of Bookpurnong data. c) Joint inversion of RESOLVE and SkyTEM data. d) Interpreted joint inversion showing shallow-conductor/mid-depth-resistor/deep-conductor sequence. All figures show cross-sections of a 3D model, and each cross-section has a vertical exaggeration of 5.

Acknowledgments

The authors acknowledge TechnoImaging for support of this research and permission to publish. M. S. Zhdanov acknowledges support from the University of Utah's Consortium for Electromagnetic Modeling and Inversion (CEMI).

<http://dx.doi.org/10.1190/segam2013-0711.1>

EDITED REFERENCES

Note: This reference list is a copy-edited version of the reference list submitted by the author. Reference lists for the 2013 SEG Technical Program Expanded Abstracts have been copy edited so that references provided with the online metadata for each paper will achieve a high degree of linking to cited sources that appear on the Web.

REFERENCES

- Cox, L. H., G. A. Wilson, and M. S. Zhdanov, 2010, 3D inversion of airborne electromagnetic data using a moving footprint: *Exploration Geophysics*, **41**, no. 4, 250–259, <http://dx.doi.org/10.1071/EG10003>.
- Cox, L. H., G. A. Wilson, and M. S. Zhdanov, 2012, 3D inversion of airborne electromagnetic data: *Geophysics*, **77**, no. 4, WB59–WB69, <http://dx.doi.org/10.1190/geo2011-0370.1>.
- Cox, L. H., and M. S. Zhdanov, 2007, Large scale 3D inversion of HEM data using a moving footprint: 77th Annual International Meeting, SEG, Expanded Abstracts, 467–470, doi: 10.1190/1.2792464.
- Cox, L. H., and M. S. Zhdanov, 2008, Advanced computational methods for rapid and rigorous 3D inversion of airborne electromagnetic data: *Communications in Computational Physics*, **3**, 160–179.
- Hursán, G., and M. S. Zhdanov, 2002, Contraction integral equation method in three-dimensional electromagnetic mode ling: *Radio Science*, **37**, no. 6, RS002513, <http://dx.doi.org/10.1029/2001RS002513>.
- Zhdanov, M. S., 2002, *Geophysical inverse theory and regularization problems*: Elsevier.
- Zhdanov, M. S., 2009, *Geophysical electromagnetic theory and methods*: Elsevier.